EVALUATION OF DESIGN CRITERIA FOR SQUIRREL CAGE FANS USED IN PUBLIC TRANSPORT HVAC SYSTEMS

ABSTRACT

This paper completes a thorough review of the leading squirrel-cage fans, currently used for HVAC urban transport units, in terms of geometry and both aerodynamic and noise performance. Based on twin-impeller, forward-curved centrifugal configuration, a benchmarking with up to 15 different commercial units from several manufacturers has been carried out in this study, ranging most significant geometrical and operational parameters for comparison. Experimental data concerning best-efficiency points, overall efficiency range, noise generation and performance has been obtained in a test facility built according to standardized industrial normative. The analysis of the obtained results is applied to select the best alternatives among those analysed, focusing on energy efficiency and minimum noise generation criteria. In this way, the most important design criteria are established in order to get more efficient and less noisy ventilation systems.

INTRODUCTION

The design of fans for HVAC applications in public transport is nowadays based on benchmarking practices between the leading manufacturers worldwide. Focused on the economical aspects rather than innovating on new concepts, the current designs are typically based on tiny modifications over well-mature, finished products, leading to an oversupply of similar small fan units in the global market. At this point, a reformulation of the basic parameters required for new designs and the proposal of practical guidelines for manufacturers become really necessary to improve the overall R&D cycle in the near future.

Small centrifugal and axial fans are used in automobile applications. In particular, a specific type of centrifugal fans named "squirrel-cage" is broadly used in these systems. Their main geometrical characteristics are a large number of short chord forward-curved blades, and a rotor exit-to-inlet area ratio unusually large (Kind and Tobin, 1990). Due to its size and relative high specific speed, these fans are used in applications with requirements of compact size, high flow rate and low cost. Typically, these fans are used to work at high rotation speed (over 4000 rpm) and variable operation conditions, even at extreme off-design points. Flow instabilities, low efficiency and high levels of noise and vibrations appear in these machines due to these working characteristics and to the need for low fabrication costs. A basic feature of their impellers is the deficient flow guiding, as a result of the short radial length of the blades and their strong curvature. This effect is counterbalanced by a greater number of blades. Such an arrangement can cause the flow to stall, even at design conditions. Cau et al. (1987) showed in their work that the poor design of the flow channel in these fans causes a severely distorted primary flow, with early flow separation on the suction side at both low and design flow rates. They ascribed the inefficiencies of these machines to the sharp axial-to-radial bend, the large inlet gap between inlet nozzle and impeller shroud and poor matching between impeller outlet and volute tongue.

This paper completes a thorough review of commercial squirrel-cage fans from leading manufacturers in terms of geometry and both aerodynamic and noise performance. Based on twin-impeller, forward-curved centrifugal configuration, a benchmarking with 15 different commercial units has been carried out in this study, ranging most significant geometrical and operational parameters for comparison. Experimental data concerning best-efficiency points, overall efficiency range, noise generation and performance have been obtained in a test facility built according to standardized industrial normatives.

Basic geometrical characteristics and best-efficiency points have been correlated in order to match performance variables with design parameters. Special attention has been paid on the optimal values required to minimize flow disturbances, to reduce the impeller-volute interaction and control the noise generation. A detailed classification of the different factors affecting the overall trend for the performance curves is also provided for every family of centrifugal fans tested, trying to identify the impact of every single parameter on the global behaviour of the fans.

GENERAL DESCRIPTION OF THE MACHINES

All the turbomachines studied here consist of two squirrel cage fans at each side of an electrical engine. They are commonly used as part of the evaporator in air-conditioning systems for public transport (Figure 1). The fans blow the cooled air into the canalization that delivers fresh air towards the passengers inside the cabin.

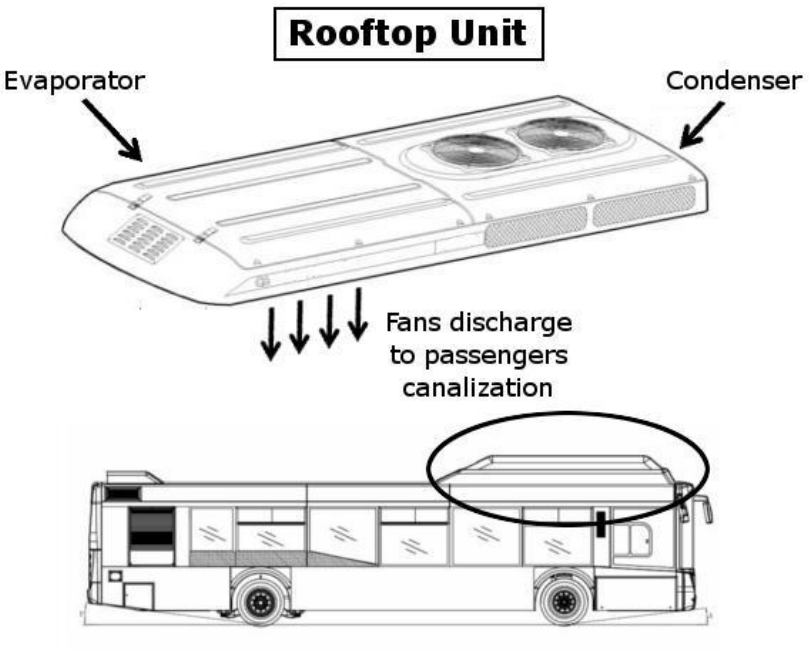

Figure 1: Rooftop unit of air-conditioning system

A generic fan configuration is shown in Figure 2. A fan casing volute comprises two impellers, which are further joined to a second module placed behind the electrical motor.

Hence, each impeller has two sets of a large number of short chord forward-curved blades separated by a central plate. The discharge sections are rectangular, while the aspirations sections are circular. Due to this configuration, these machines present two differenced inlets: two free inlets, one on each side of the fan, and two partially obstructed ones on the sides close to the electrical engine. All these facts lead to the appearance of non-symmetric inlet flow conditions.

Note that the presence of the central plate is introduced to reduce the air recirculation at the inlet (Eck, 1973). Moreover, it is a common practice to let the blades of each half lie half-way between those of its counterpart impeller, in order to minimize the noise component related to the tonal BPF.

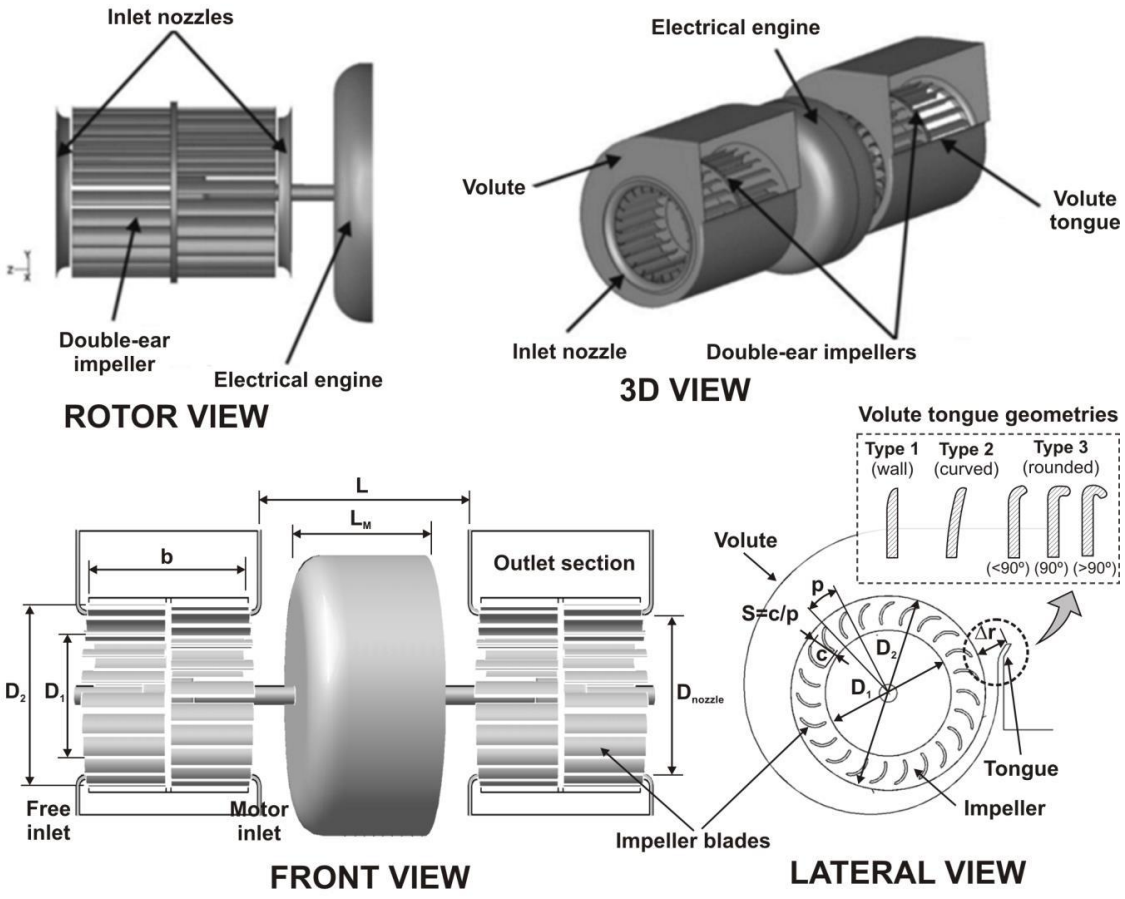

Figure 2: Generic Squirrel-Cage fan configuration: Three-dimensional sketch and basic geometrical parameters.

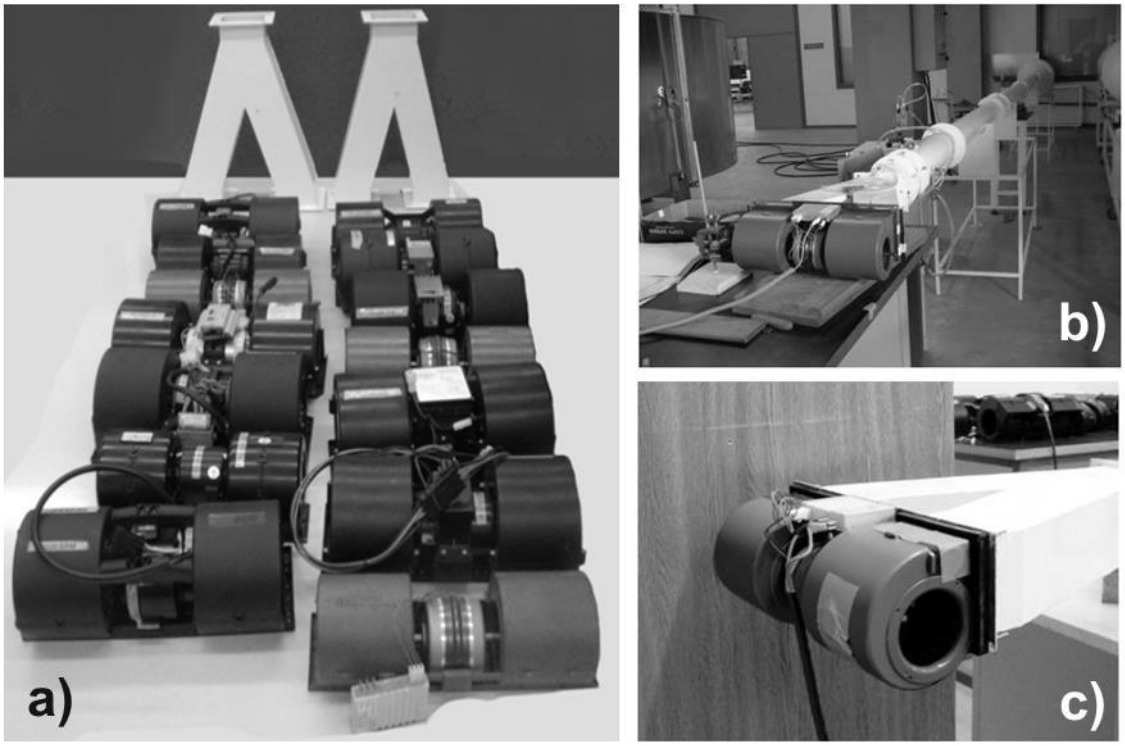

Figure 3: a) Tested fans and Y-shaped ducts. b) Typical arrangement for performance tests. c) Detail of the ventilation unit connected to the Y-shaped duct.

METHODOLOGY

First, a detailed description of geometric and construction parameters of the available equipment have been made. This data collection includes diameters (impeller inlet, impeller outlet and inlet nozzle), widths (impeller and volute), thicknesses, numbers of blades, impeller-volute distances, volute inlet configurations, drive systems and building materials. Figure 3 shows the different squirrel-cage fans analysed and two of the Y-shaped ducts (a) used for the connection to the testing facility. Also, a global view of the facility (b) and a detail of the ventilation unit connected to a Y-shaped duct are provided (c).

The tests for the aerodynamic and acoustic characterization of the fan have been made in a normalized ducted installation (type B, according to ISO 5801 and ISO 5136). Figure 4 shows a sketch of this test facility. The flow leaving the two impellers is merged in a Y-shaped duct placed immediately downstream the outlet section. After leaving the fan, the air flows through

a straightener in order to remove the swirl component generated by the fan. At the end of the facility, an anechoic termination removes undesired noise reflections and a regulation cone permits to modify the fan operating point.

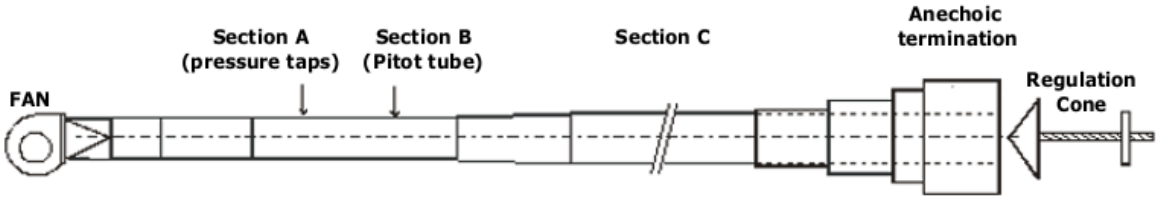

Figure 4: Sketch of the test installation

More details about the followed procedures can be found in Velarde-Suarez et al. (2008). The tests were conducted at a constant voltage of 26.5 V for the electrical motor, which is a typical value during the operation of the fans in the air-conditioning system. The performance curves were obtained measuring between seven to eight points for the whole operating range of the fans, which was considered accurate to describe their overall characteristics. At each of these points, several physical parameters were measured: static pressure (Section A), dynamic pressure (Section B), electrical engine voltage and current intensity, rotation speed and acoustic pressure in the duct. Air temperature and density in the laboratory were also recorded at the beginning of each fan characterization.

The acoustic pressure measurements have been made using two 1/2” microphones. The uncertainty of the microphones is declared by the manufacturer in 0.2 dB, with a confidence level of 95%. The signal from the microphone preamplifiers is introduced in a 2-channel real-time acquisition unit, which software is afterwards employed to postprocess the measured signals. Consequently, Lp spectrums, both inside the duct (Section C) and outside the fan (in a point located 0.5 m upstream the fan inlet), were retrieved using this procedure, typically with the microphone aligned to the impeller shaft.

RESULTS AND DISCUSSION

Morphological results

All the volutes and the impellers of the fans analysed are made of plastic materials, except for just one impeller made of aluminium (named F01 in the database). On the contrary, there is a noticeable difference between the stiffness of the plastic materials used in the construction of the impellers. In addition, nine out of fifteen impellers have 28 blades; other three have 34 blades and the last three fans have 23, 24 and 26 blades respectively.

Table 1: Maximum and minimum values of significant measured parameters

	ψ	**Φ**	**n_s**	**d_s**	**D_{nozzle}/ D_1**	**D_1/ D_2**	**$4b/D_1$**	**$\Delta r/D_1$ [%]**	**ω [rpm]**	**S**
Max	0.36	0.26	3.00	1.42	1.22	0.85	3.10	22.50	5170	1.58
Min	0.14	0.17	1.47	0.80	0.95	0.71	2.05	12.12	3580	0.88

Concerning other geometrical parameters, the ratio of the inlet nozzle diameter to the impeller inlet diameter (D_{nozzle}/ D_1), the inner-outer diameter ratio (D_1/D_2), the aspect ratio between the outlet width and the inner diameter ($4b/D_1$), the impeller-tongue radial distance ($\Delta r/D_1$) and the solidity (S) have been summarized for the entire database. All the dimensionless parameters are calculated for the best efficiency point. The fans present important differences in diameters and impeller widths so the authors have considered "bD^2" as the characteristic dimension in the flow coefficient instead of "D^3".

Table 1 shows the maximum and minimum values for these representative parameters in the study, as well as additional operational information. Table 2 summarizes the morphological

parameters for all the models studied, ranged by specific speed. The different types of tongue shapes are illustrated in figure 2.

Table 2. Morphological parameters

	D_1 [mm]	D_{nozzle}/D_1	D_1/D_2	$4b/D_1$	L_m/L	Z	S	$\Delta r/D_1$ [%]	Tongue shape (types)	Rotor stiffness
F01	82	0.95	0.85	2.05	0.75	34	0.92	20.8	1 (rounded)	rigid (alum.)
F02	77	1.01	0.78	2.31	0.86	28	1.27	12.1	1 (straight)	rigid
F03	76	1.03	0.77	2.34	0.77	28	1.35	13.1	1 (rounded)	soft
F04	76	1.00	0.77	2.34	0.93	28	1.35	15.2	3 (>90º)	rigid
F05	74	1.05	0.77	2.35	0.67	28	1.32	17.7	1 (straight)	rigid
F06	71	1.14	0.84	3.10	0.61	28	0.88	16.5	3 (<90º)	rigid
F07	65	1.09	0.77	2.58	0.71	26	1.21	19.0	1 (rounded)	rigid
F08	77	1.01	0.79	2.29	0.86	28	1.22	15.3	1 (rounded)	semi-rigid
F09	58	1.21	0.71	3.03	0.75	24	1.58	12.2	1 (straight)	semi-rigid
F10	80	1.13	0.82	2.23	0.55	34	1.15	15.5	3 (90º)	soft
F11	80	1.00	0.82	2.23	0.55	34	1.15	18.6	3 (90º)	semi-rigid
F12	75	1.03	0.77	2.35	0.86	28	1.31	17.5	1 (rounded)	semi-rigid
F13	60	1.10	0.75	3.00	0.65	23	1.22	22.5	3 (90º)	semi-rigid
F14	76	1.22	0.78	2.34	0.87	28	1.29	20.4	2 (curved)	soft
F15	76	1.01	0.78	2.34	0.68	28	1.29	17.3	2 (curved)	soft

An important design parameter in this type of fans is the ratio between the diameters of the inlet nozzle and the impeller inlet (D_{nozzle}/ D_1). The presence of a "no-flow" zone over the impeller blades near the inlet can be noticed. In the region over the impeller blades near the inlet, there is little or no through-flow and the blade passages contain completely separated flow (Kind and Tobin, 1990). In this zone, high axial momentum dominates the inlet flow and the static pressure distribution in the hub is not enough to turn the flow in the radial direction. Due to the existence of this separated region, the volute flow varies significantly with axial location. There is a first zone, near the volute inlet, where the flow has a predominant tangential component and a second area, at the midspan and central plate, where the radial component dominates the flow. In this type of fan, it is common to choose $D_{nozzle}/D_1 > 1$, in

order to facilitate the incoming flow to the impeller, minimizing the flow separation zone observed in

Figure 5. A sketch of the separated flow developed at the inlet, adapted from Kind and Tobin (1990), is illustrated at the left side of the figure. At the right, numerical results from a URANS, CFD modeling of the F13 fan, are also included (from Ballesteros-Tajadura et al., 2009), confirming this detrimental effect at maximum flow rates.

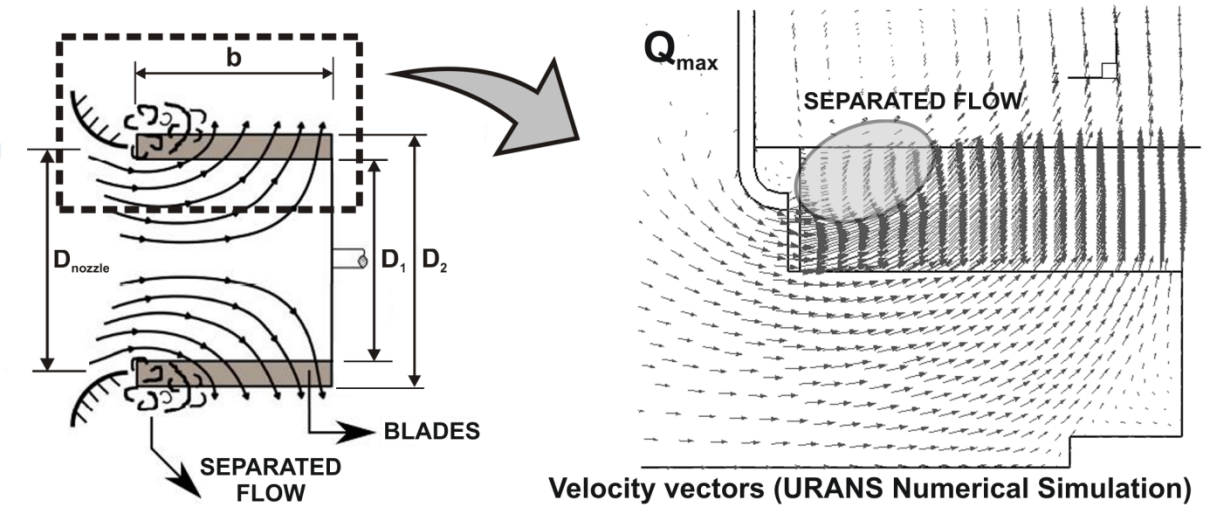

Figure 5: a) Separated flow in the impeller inlet (adapted from Kind and Tobin, 1990). b) Numerical results from URANS simulation: velocity vectors showing the inlet separation (from Ballesteros-Tajadura et al., 2009).

As it is shown in Figure 6, the ratio between the inlet and outlet diameters of the impellers presents an almost constant value around 0.78 for most of the fans. Only a reduced number of manufacturers have chosen to design the impeller with a higher ratio (F01, F06, F10 and F11). On the other hand, only two of the fans observed present a lower D_1/D_2 ratio than the previously referenced 0.78 value, which correspond to particularly small fan models (F13 and F09). The influence of this parameter over the aerodynamic performance will be discussed later.

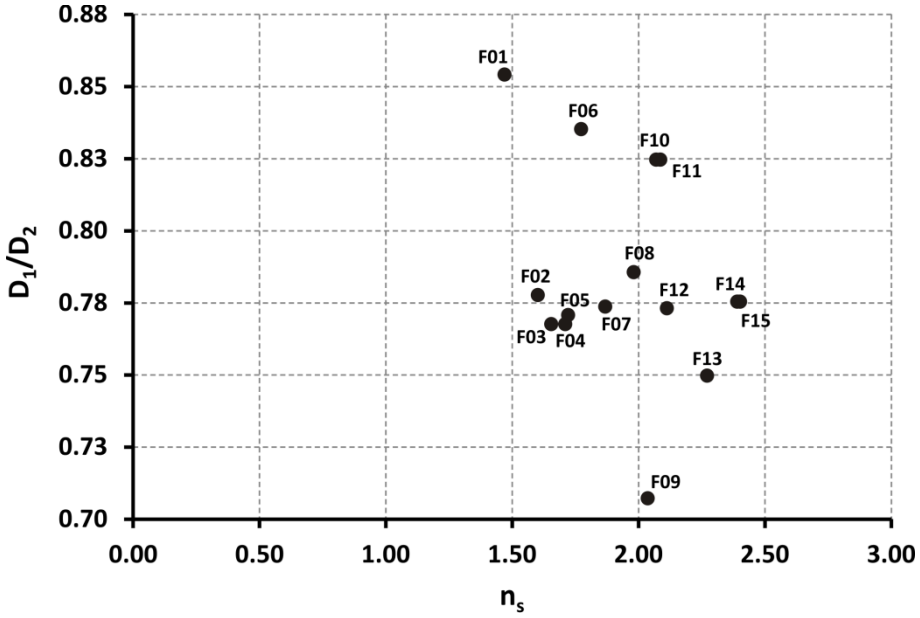

Figure 6: D_1/D_2 vs. specific speed

In Figure 7, the $4b/D_1$ parameter, which represents a way of measuring the flow uniformity at the inlet, is plotted. According to the literature, this parameter must be close to 1 to assure a uniform flow for this type of centrifugal fans. However, as can be noticed from the figure, the commercial fans analysed here present a width-to-diameter ratio unusually large, ranging between 2 and 3, far beyond optimum values. As a consequence, the fans present a recirculation zone at the inlet where the flow is separated and major flow disorder arises. Box A in Figure 7 points out those fans presenting the worst ratios (F13, F06 and F09); once again, the smallest fans (named as F13 and F09) are penalized because of their reduced inlet diameters (it is important to note that the impeller width is very similar in all the cases). In the same figure, the F01 fan is the one presenting the lowest value for this ratio, though its inlet blockage ruins its flow uniformity at the inlet.

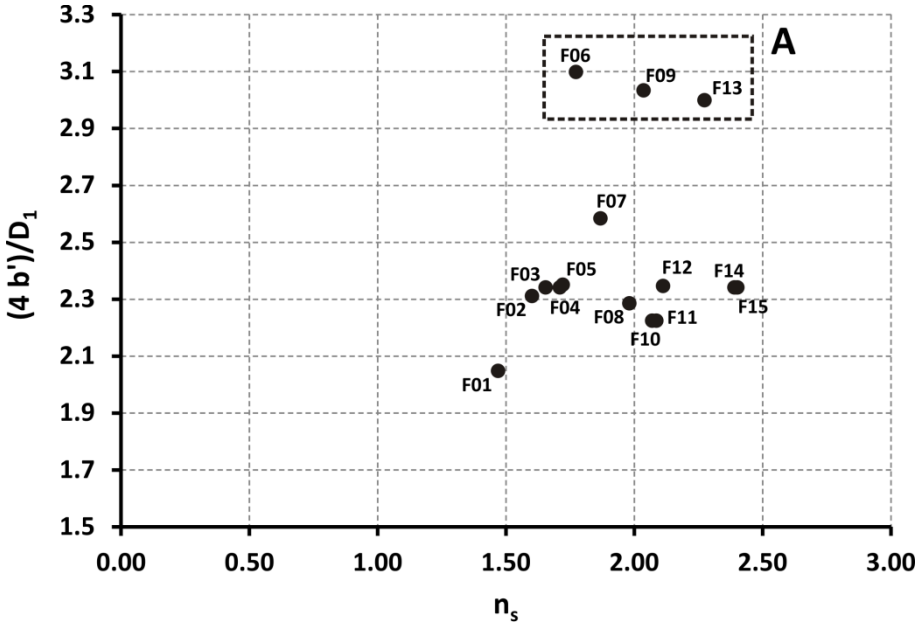

Figure 7: 4b/D_1 vs. specific speed

A solidity parameter S has been defined as the blade chord divided by the blade spacing. Backström (2009) has recommended to radial turbomachinery researchers and designers the use of solidity to correlate slip factor, that is, the rate at which centrifugal turbomachines do less work than that calculated with the assumption that the relative impeller exit flow follows the blade trailing edges. Typical values of solidity in centrifugal turbomachinery ranges from 0.5 to 2.5. In the fans analysed here, the solidity values ranges from 0.88 to 1.58, but the most frequent values are around 1.20-1.30.

Finally, Figure 8 shows the Cordier diagram for the entire database, i.e., the plot with the specific diameter d_s versus the specific speed n_s. This collection of squirrel cage fans present specific speeds ranging from 1.5 to 1.25 with specific diameters between 1 and 1.4. Additionally, an efficiency contour is plotted from the results of total efficiency showed in table 3 below. The Cordier line, which defines the correlations between specific speed and specific diameter for maximum efficiency, is also given in the figure (dashed line). Overall shape of the efficiency distributions and the Cordier line are in consonance with typical results from classical references (Balje, 1962; Csanady, 1964), thus confirming the reasonable

designs of all the squirrel-cage fans studied and advancing the recommended design regions to obtain maximum efficiencies.

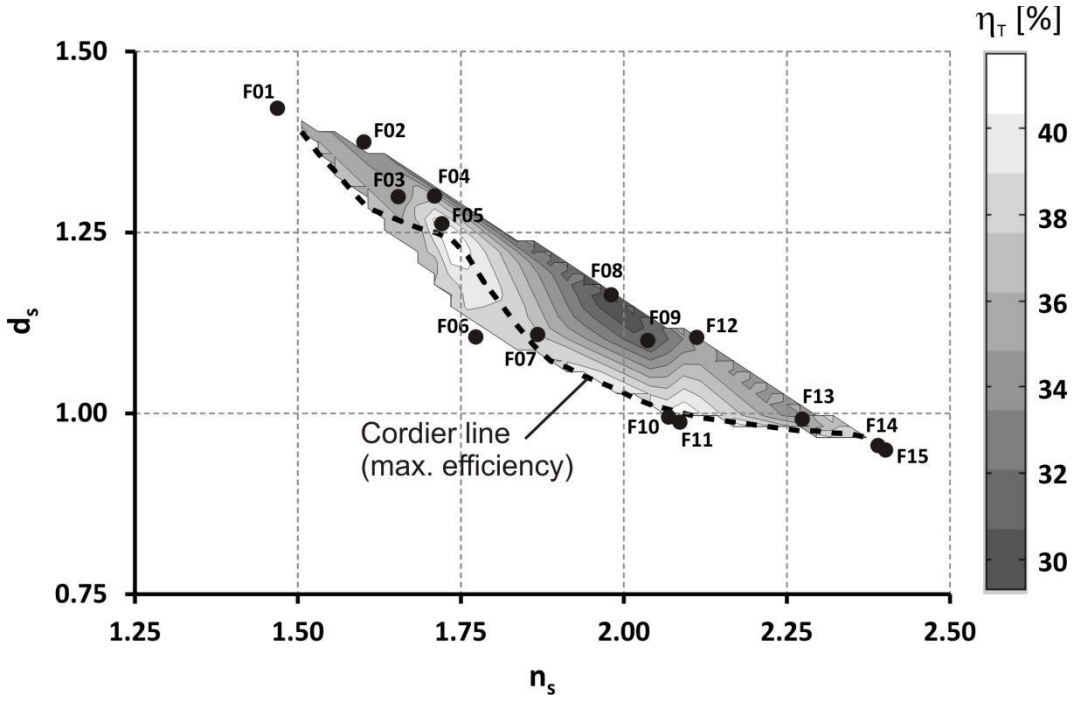

Figure 8: Cordier diagram: Specific diameter vs. specific speed

Operational results

Performance curves for three representative fans are shown in Figure 9 as an example of the results obtained during these tests. All fans present the typical performance curves associated to forward-curved blades centrifugal fans, including instability zones. In the central flow zone, a loss of pressure followed by a recovery can be noticed in all these cases. This instability, denoted by a flat or positive slope in the performance curve, is inherent to the design of forward-curved blade fans. The authors, in previous experiences, observed an increment of unstable effects with increasing rotational speed. Thus, this unstable behaviour appears to be intensified by the poor structural stiffness of the impeller blades.

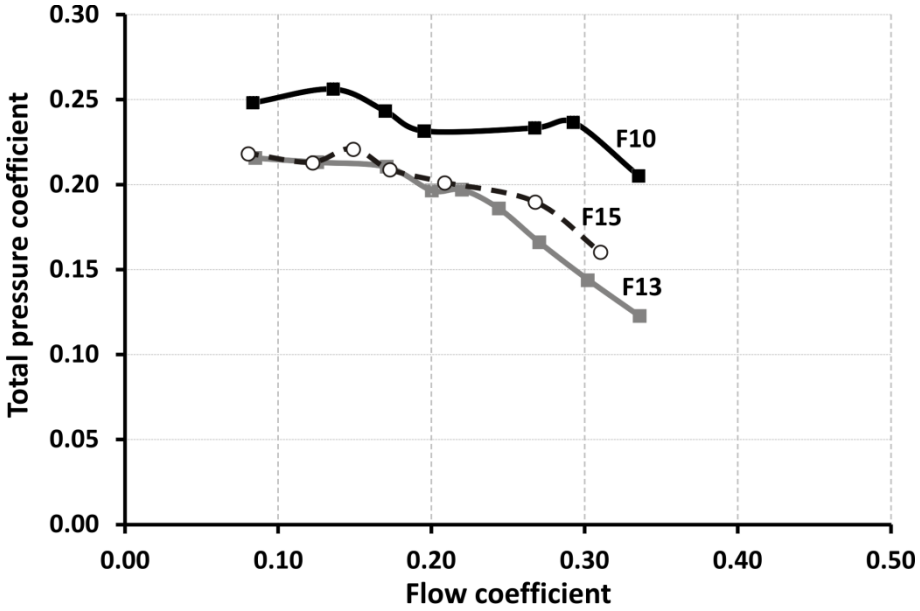

Figure 9: Performance curves for three representative fans

The most important operational parameters are listed in table 3. In particular, total pressure and delivered flow rate at nominal conditions are included for each fan. Other aerodynamic variables like the pressure and flow coefficients, the total efficiency or the specific speed and diameter are also provided. The sound pressure levels at the blade passing frequency, $Lp_{s,Z}$, is given as a representative variable of the aeroacoustic performance of the fans.

Table 3. Operational parameters at the BEP

	Q_n [m³/h]	ϕ	P_T [Pa]	ψ	n_s	d_s	η_T [%]	Lps_Z	ω [rpm]
F01	355	0.14	572	0.23	1.47	1.42	37.6	17.4	4497
F02	693	0.13	391	0.21	1.60	1.38	34.0	43.2	4351
F03	700	0.15	416	0.22	1.65	1.30	36.1	35.0	4263
F04	382	0.15	410	0.20	1.71	1.30	38.4	50.3	3930
F05	433	0.16	527	0.21	1.72	1.26	43.6	34.7	4490
F06	400	0.16	432	0.26	1.77	1.11	39.4	24.6	4141
F07	372	0.20	396	0.23	1.87	1.11	38.5	42.2	4244
F08	433	0.18	350	0.19	1.98	1.16	28.9	47.4	3806
F09	333	0.17	338	0.20	2.04	1.10	30.4	37.7	4346
F10	665	0.27	461	0.24	2.07	0.99	43.0	28.4	3940
F11	750	0.27	570	0.24	2.09	0.99	43.7	25.5	4384
F12	561	0.19	499	0.18	2.11	1.10	35.1	24.4	4646
F13	389	0.20	337	0.20	2.27	0.99	34.4	24.6	4476
F14	718	0.26	439	0.19	2.39	0.96	41.5	30.2	4220
F15	423	0.27	557	0.19	2.40	0.95	40.8	37.0	4100

In the case of this type of centrifugal fans, for a given size and rotational speed, the manufacturers are mainly focused on delivering large flow rates maintaining a total pressure as high as possible. Under this simple design criterion, it is possible to reduce the number of fans to be installed per ventilation unit, saving costs and matching pretty-close the important restrictions respect to the available room in typical rooftop arrangements (Figure 1). This implies that both electrical consumption and total efficiency, though being really important, are not as critical for the designers as it is the case of pressure and flow rate performance. Consequently, in the following, most of the comments and discussion provided in the paper are referring only to both flow and pressure coefficients.

Figure 10 shows the relationship between total pressure and flow coefficients at the best efficiency point (BEP) for the different turbomachines. The flow coefficient and the total pressure coefficient are bounded between 0.14–0.2 and 0.18–0.27 respectively. Only four of the tested fans (F10, F11, F15 and F14) reached a higher flow coefficient (around 0.27). Among them, F10 and F11 are those with the highest pressure coefficients, so they can be considered as the most interesting fans in the benchmarking. These two models present very low values of width-to-diameter ratio, which becomes an advantage when competing to provide an extra flow rate. This confirms again the strong influence of this parameter to obtain a good performance. Only F01 model presents a lower width-to-diameter ratio, but it fails in other critical aspects, as commented below.

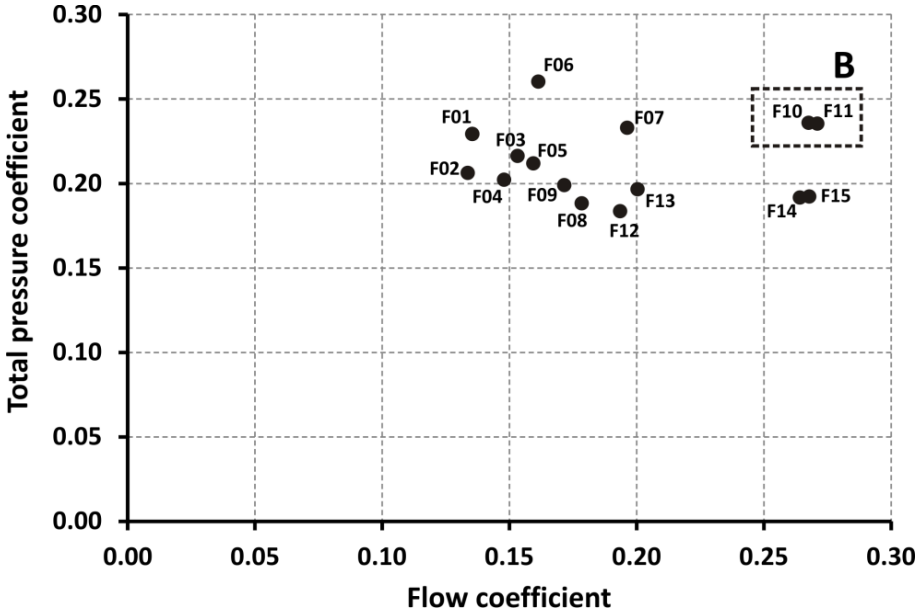

Figure 10: Total pressure coefficient vs. flow coefficient at the BEP

Furthermore, models F10 and F11 stand out also for the ratio between inlet and outlet diameters, D_1/D_2, with the highest values in the analysis (significantly larger than the typical value 0.78 from the other fans). In previous section, it was shown that the models F06 and F01 also presented significant large values of D_1/D_2. However, the aerodynamic performance of these two last fans is seriously compromised due to the unfortunate selection of other parameters. In particular, the F09 unit presents the worst width-to-diameter ratio in the analysis and F01 presents a ratio $D_{nozzle}/D_1 < 1$ and an unusual large motor placed too close to the aspirating section.

Concerning the D_{nozzle}/D_1 ratio, it was previously established that it should be fixed to values above unity. In order to determine the optimal value for this parameter, a fan very similar to the F13 model, with the possibility to introduce inlet nozzles of different diameters, has been tested. Hence, figure 11 shows the obtained results for the pressure coefficient and the overall efficiency as a function of the flow coefficient when three different D_{nozzle}/D_1 ratios (1, 1.10 and 1.13) are considered. Effectively, it is observed a remarkable improvement of the pressure and efficiency curves when the D_{nozzle}/D_1 is above unity, especially at middle and high flow

rates. On the contrary, no relevant differences can be reported in the performance for the results obtained with ratios of 1.10 and 1.13.

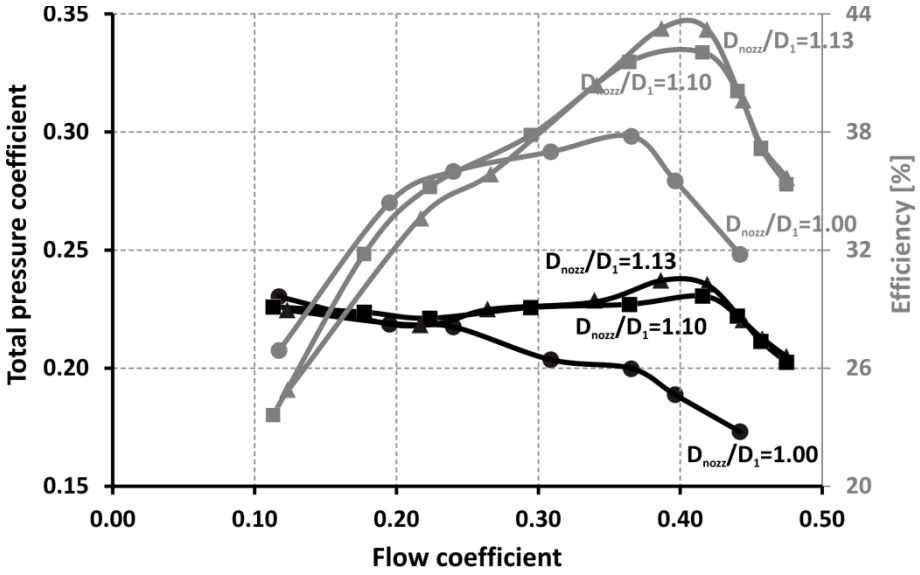

Figure 11. Influence of the parameter D_{nozzle}/D_1 on the performance curves.

Fans F10 and F012, with the higher pressure and flow coefficients, have been designed with a solidity value of 1.15, in the mid range of this parameter in the present study. According to Backström (2009), higher values of solidity are related to a better guiding of the flow by the blades, and thus to an effective impeller work closer to the theoretical one (that is, assuming that the relative impeller exit flow follows the blade trailing edges). However, an important increment in the impeller solidity would generate at the same time increasing aerodynamic losses in the blade channels, so there is a need for a compromise in order to found an optimized value of solidity parameter: not too low in order to obtain optimum guiding of the flow, and not too high in order to minimize aerodynamic impeller losses. In the present study, this optimized solidity value appears to be around 1.15-1.30.

Additionally, the two best-designed fans, previously mentioned as F10 and F11, are the ones presenting total efficiency values (η_t) exceeding 40%. However, it must be noted that these

values of total efficiency include the motor-fan consumption. Therefore, to achieve good values in the overall performance is important to have also a good electric motor; it is not enough to optimize exclusively the aerodynamic design of the fan.

Precisely, another geometric parameter with a relevant influence on the aerodynamic behaviour of the fan is the relative size of the driven motor respect to the impellers. It has been observed that all the analysed motors present a diameter very similar to that of the fan inlet, but with notable variations respect to their lengths. Consequently, table 2 also provides the ratio L_M/L between the motor length and the total axial separation between the two impellers of the fan (figure 2). Figure 12 summarizes the correlation between this parameter and the total efficiency, revealing a decreasing trend in the efficiency as the motor size is enlarged.

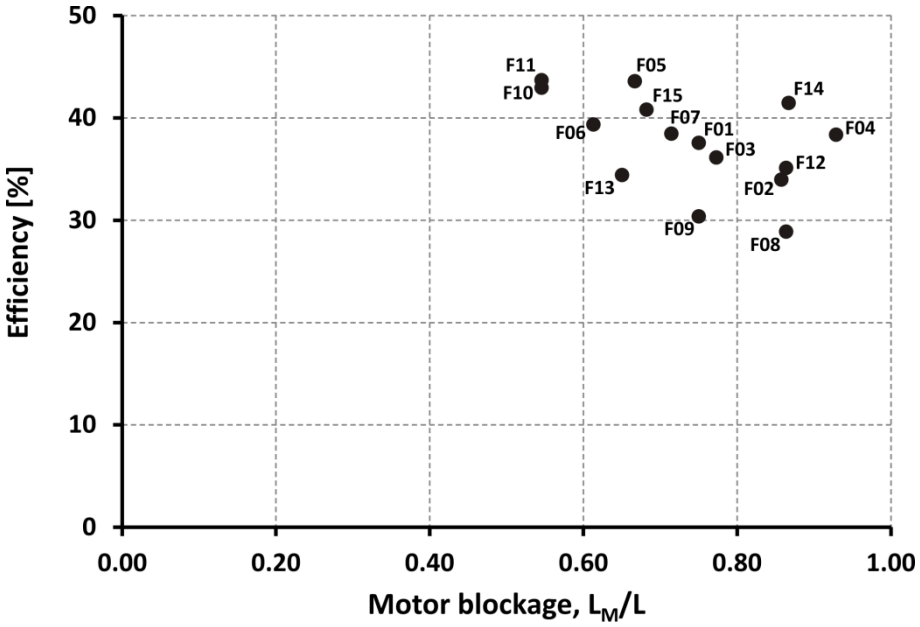

Figure 12. Total efficiency vs L_M/L

To provide a better evidence of this trend, a fan very similar to the F13 model, but driven with an external motor, has been tested with a set of cylindrical pieces of different sizes that mimic the aerodynamic blockage of the motor. In particular, figure 13 shows once again the pressure

coefficient and the efficiency as a function of the flow rate coefficient for three different configurations: free aspiration (with no pieces interfering the impellers inlet) and pieces pretending a motor blockage of L_M/L=0.65 and 0.75, respectively. The figure shows the notable improvement associated to a reduction of the motor size. As an order of magnitude, it can be affirmed that with a motor size reduction of a 15% (i.e. from 0.75 to 0.65), the flow and pressure coefficients are increased a 4% and a 6.8% respectively at the best efficiency point, which in turn it is also improved in 2.1 points (from 33.5 to 35.6%).

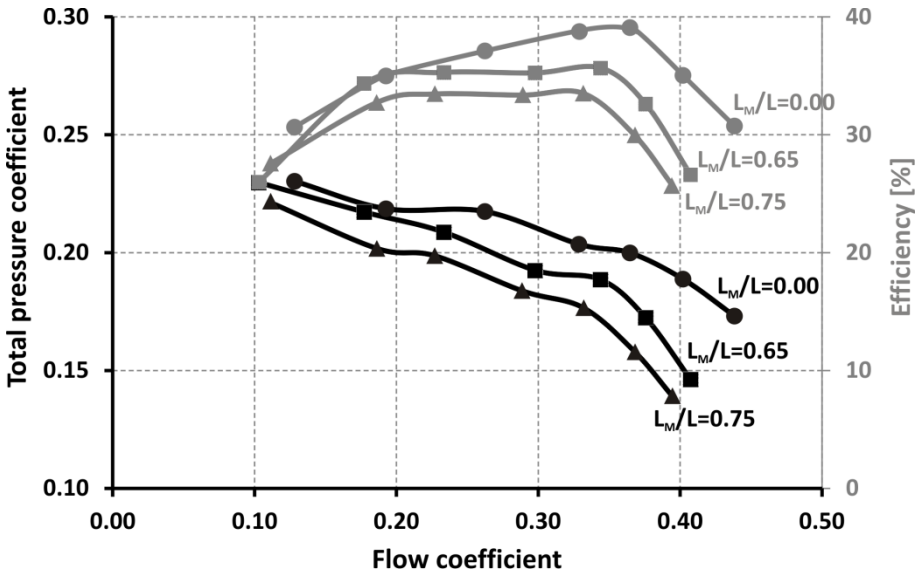

Figure 13. Influence of the parameter L_M/L on the performance curves

Acoustic results

In order to compare the sound pressure levels of fans with different sizes and performance parameters, the specific sound pressure level parameter Lp_s has been calculated as indicated in Equation 1.

$$Lp_s = Lp - 10\log_{10}(Q) - 20\log_{10}(P_T) \qquad (1)$$

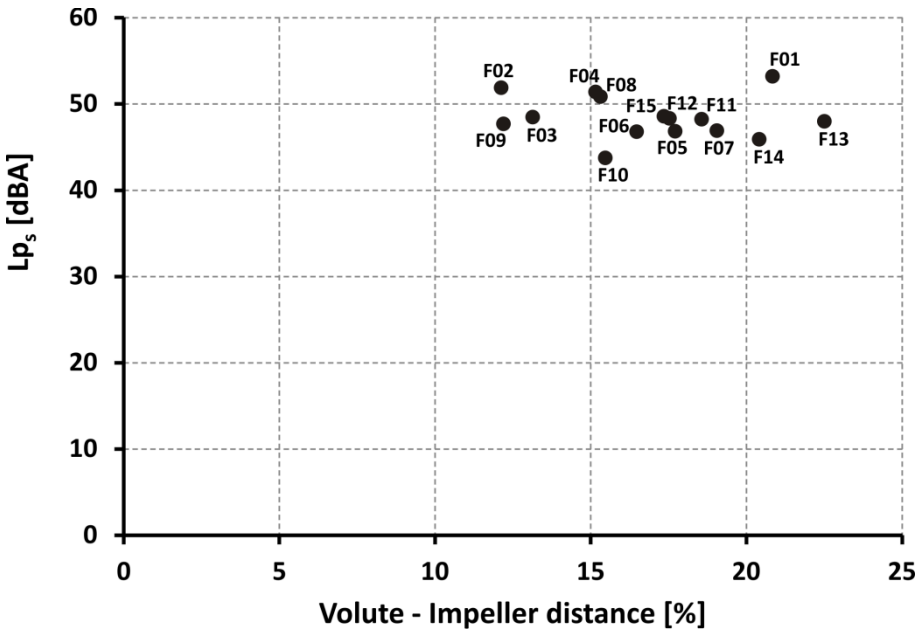

Figure 14. Lp_s vs. volute-impeller distance at the BEP

This parameter takes into account the operation point of the machine, the flow and the total pressure, when the noise level is measured. Figure 14 represents the total sound pressure level measured at the best efficiency point versus the distance between volute and impeller ($\Delta r/D_2$). The results do not show the expected trend, since, as pointed by Velarde-Suárez et al. (2008), a reduction of the distance between volute and impeller should imply a drop in the sound levels of the fans. But looking at the figure, no relationship between the volute-impeller distance and the noise levels can be expected. This is due to the fact that the total Lp_s includes various noise sources. These sources include aerodynamic noise, mechanical noise generated by the fan and the noise produced by the electric motor. Cory (1992) has summarised all the possible sources of fan noise. According to this author, for centrifugal fans, where the motor is usually outside the airstream, electromagnetic noise will not contribute to the in-duct sound power level. It may, however, mask the radiated noise from the fan casing and ducting system. Also, mechanical sources of noise may constitute an important contribution to the total acoustic generation in this kind of machines. In particular, when the fan operates at a

range of rotational speeds, it may be subject to resonances in some components, which whilst insufficient to cause failure, may lead to an unforeseen increase in noise at a particular speed.

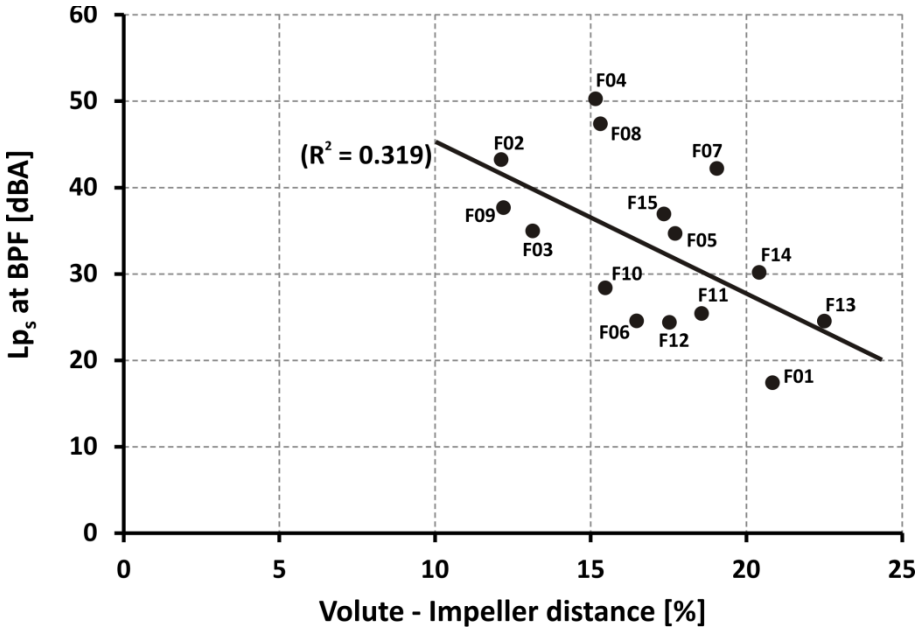

Figure 15. Lp_s at the BPF vs. volute-impeller distance at the BEP

In order to analyse only the aerodynamic tonal noise, figure 15 shows the noise levels at the blade passing frequency for the studied machines when operating at their best efficiency point. Indeed, taking into account only the tonal component of the noise generated, there is a downwards trend in the noise levels captured when the distance between volute and impeller is increased, confirming previous results cited above. It is widely known that the human ear does not respond equally to the sound frequency. The human ear is very sensitive to sounds with frequencies around 1000-2000 Hz. In all the studied fans, the blade passing frequencies fall in this range, so the aerodynamic tonal noise constitute an annoying contribution to the total noise generation.

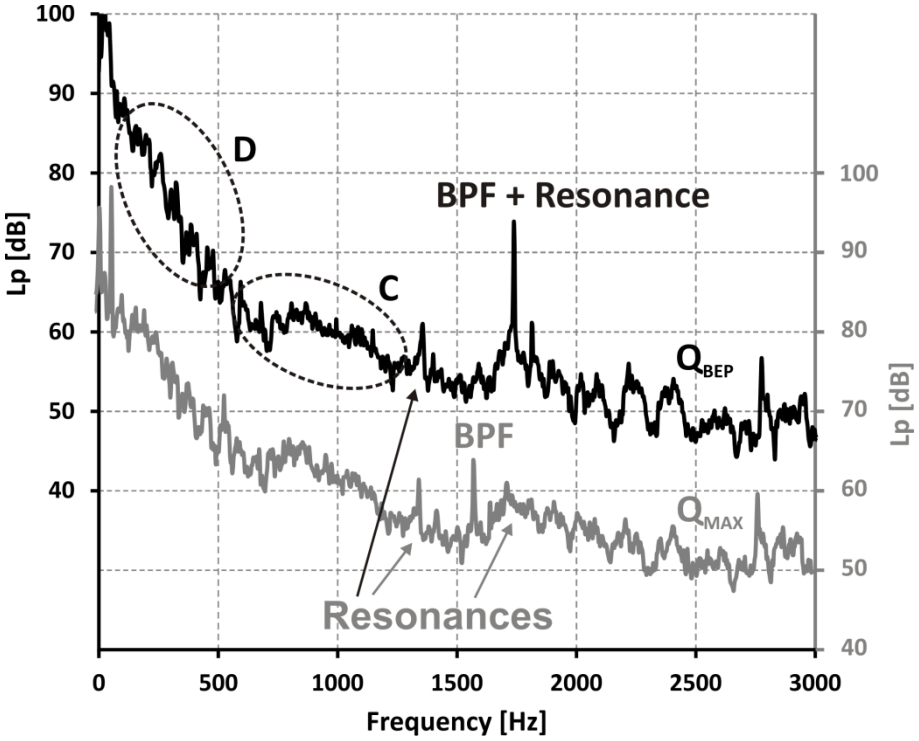

Figure 16. Lp spectra for the fan F13

Figure 16 represents the Lp spectra obtained with the microphone placed inside duct, at two different flow rates for the fan F13. It is important to note that all these fans are driven at constant voltage, in similar fashion to the real conditions within the rooftop units of the buses. This fact implies a variable rotational speed that it is therefore a function of the flow conditions. As a consequence, some characteristic frequencies (i.e. the BPF) exhibit small lags between the two operating points shown in the figure.

Concerning the shown spectra, it is quite remarkable the very complex patterns configuring the traces shown in Figure 16, with tonal and broadband contributions. The blade passing frequency is clearly noted as the most important tonal noise source (1736 Hz for the best efficiency point and 1577 Hz for the maximun flow rate). According to Neise (1976), this tonal source is caused by the interaction between the mean flow leaving the impeller and the fan casing. The main source region can be located at the volute tongue which is nearest to the rotating impeller blades. Velarde-Suárez et al. (2009) presented an aeroacoustic study on a

small squirrel-cage fan for public transport. They found that the predominant tonal component in the noise generation of this fan is the blade passing frequency. They noticed that the relevant values of the blade passing levels in these cases could be explained by the high pressure fluctuation values found, not only close to the volute tongue, but also in the rest of the volute. This fact is probably due to the size restrictions commonly suffered by these devices, which constitute a clear limitation on the volute design.

Regarding Figure 16, another important consideration is the existence of an area of high broadband noise for mid frequencies. The aerodynamic broadband noise is attributed by Neise (1976) to the turbulent flow acting on the solid surfaces of the impaller as well as of the fan casing. Another contribution comes from the vortex shedding at the impeller blade trailing edges. The sound radiation from the turbulent fluctuating quantities in the flow itself is presumed to be of minor importance since the mean flow Mach numbers involved are negligible. Velarde-Suárez et al. (2008) found peak contributions at frequencies not dependent on the flow conditions. They suggested that these peaks could correspond to resonance frequencies of the fan, due to the vibration of some components. A similar behaviour can be observed in the spectra shown in Figure 16. The contribution at 1350 Hz with the same value for the two flow rates appears to be caused by a component resonance. At the maximum flow rate, another resonance peak is shown at 1730 Hz. This circumstance turns out to be very unfavourable at the best efficiency point, since both tonal aerodynamic noise and frequency of resonance coincide and their effects are reinforced. This effect, as stated by Cory (1992), can explain the reason of the anomalous high level of the tonal blade passing noise at the best efficiency point.

Finally, there are also high levels of noise at low frequencies. This low-frequency noise is typical of in-ducts measurements and does not appear when the measurements are made outside the test bench.

CONCLUSIONS

In this paper, a comprehensive study of the geometric characteristics, as well as an operational and acoustic characterization of several small squirrel-cage fans, used in the evaporation system for HVAC applications in public transport, was conducted. This type of turbomachines has revealed to be quite complex with both aerodynamic and acoustic behaviours being influenced by many factors.

Different design considerations for improving performance in terms of flow parameters have been determined. The best aerodynamic performances have been observed in those fans with low values of the $4b/D_1$ parameter (in the range of 2.2), combined with a high ratio of D_1/D_2 (around 0,8). The D_{nozzle}/D_1 parameter must have values above unity to avoid a blocking design of the inlet. In particular, the present analysis reveals that it is sufficient to adopt a diameter ratio, $D_{nozzle}/D_1=1.1$, slightly higher than 1. A motor size reduction of roughly a 15% provokes that the flow and pressure coefficients are increased around a 4% and a 6.8% respectively at the best efficiency point, which in turn it is also improved in 2.1 points.

The acoustic results show different phenomena. One of them is the existence of high levels of broadband turbulent noise for mid-range frequencies. Also, it has been reported in the literature significant noise sources that may be related to the mechanical resonances of some components. High levels of noise at low frequencies in the in-duct measurements were also noticed. Considering only the tonal aerodynamic noise, specifically the one produced at the blade passing frequency, a relationship between the noise and the volute-impeller distance can be established, resulting in lower noise levels when the volute-impeller distance is increased. This design parameter must be particularly taken into account because of two reasons: Firstly, because the tonal noise at the blade passing frequency is generated at high frequencies (between 1000 and 2000 Hz), which are especially disturbing for humans; and secondly,

because at some particular rotational speeds, it may produce couplings with some kind of natural, resonance frequencies, leading to a considerable increment of the noise sources and a reduction in the passengers' comfort.

NOMENCLATURE

b = impeller width (m)

BPF = blade passing frequency

D = diameter (m)

d_s = specific diameter $\left(\frac{D_2 \cdot \left(\frac{P_T}{\rho}\right)^{1/4}}{Q^{1/2}}\right)$

Lp = sound pressure level (dB)

f = frequency (Hz)

n_s = specific speed $\left(\frac{\omega \cdot Q^{1/2}}{\left(\frac{P_T}{\rho}\right)^{3/4}}\right)$

p = static pressure (Pa)

p_0 = reference acoustic pressure (20 μPa)

P = pressure (Pa)

Q = flow rate (m^3/h)

S = solidity $\frac{\frac{D_2 - D_1}{2}}{\pi \cdot \left(\frac{D_1}{z}\right)}$

W = power consumption (W)

z = number of blades

Δr = distance between volute tongue and impeller periphery (m)

Greek Letters

ρ = density (kg/m^3)

ω = angular velocity (rpm)

ψ = total pressure coefficient $\left(\frac{P_T}{\rho\omega^2 D_2^2}\right)$

η = efficiency

Φ = flow rate coefficient $\left(\frac{Q}{\omega D_2^2 b}\right)$

Superscripts and Subscripts

1 = impeller inlet

2 = impeller outlet

BEP = best efficiency point

max = maximum

s = specific

T = total

REFERENCES

[1] Backström, T.W.von., – *A Unified Correlation for Slip Factor in Centrifugal Impellers*, Journal of Turbomachinery, Vol. 128, pp. 1–10. **2009.**

[2] Ballesteros-Tajadura, R., Guerras Colon, F.I., Velarde-Suarez, S., Fernández Oro, J.M., Argüelles Diaz, K.M., Gonzalez, J., - *Numerical model for the unsteady flow features of a*

squirrel cage fan, Proceedings of the ASME Fluids Engineering Division Summer Meeting, 2, pp. 173-183, doi 10.1115/FEDSM2009-78479. **2009.**

[3] Balje, O., - *A Study on Design Criteria and Matching on Turbomachines*, ASME J. Eng. Power, 84, pp. 103-114, **1962.**

[4] Cau, G., Mandas, N., Manfrida, N. and Nurzia, F., – *Measurements of primary and secondary flows in an industrial forward-curved centrifugal fan*, ASME J. Fluids Eng., 109, pp. 353-358. **1987.**

[5] Cory, W.T.W., - *Acoustic similarity laws for the prediction of industrial fan sound levels*, Proceedings of FAN NOISE Symposium, pp. 305-328, Senlis, France, **1992**.

[6] Csanady, G.T., - Theory of Turbomachines, Ed. Mc-Graw Hill, New York, **1964.**

[7] Eck, B., – *Fans, Design and operation of centrifugal, axial-flow and cross-flow fans*, Pergamon Press Ltd. **1973.**

[8] International Organization for Standarization *ISO 5136:1990 and Technical Corrigendum 1:1993. Determination of sound power radiated into a duct by fans. In-duct method*. **1990.**

[9] International Organization for Standarization *ISO 5801: 2007. Industrial fans-Performance testing using standardized airways*. **2007.**

[10] Kind RJ, Tobin MG., *Flow in a centrifugal fan of the squirrel cage type*, ASME J Turbomach, 112:84–90, **1990**.

[11] Velarde-Suárez S, Ballesteros-Tajadura R., Pereiras-García, B., Santolaria-Morros, C., – *Reduction of the aerodynamic tonal noise of a forward-curved centrifugal fan by modification of the volute tongue geometry*, Applied Acoustics, Vol. 69, pp. 225–232. **2008.**

[12] Velarde-Suárez S, Ballesteros-Tajadura R, González, J., Pereiras-García, B., – *Relationship between volute pressure fluctuation pattern and tonal noise generation in a squirrel-cage fan*, Applied Acoustics, Vol. 70, No. 11-12. , pp. 1384-1392. **2009.**